

# ACCOUNTS of CHEMICAL RESEARCH®

FEBRUARY 2003

Registered in U.S. Patent and Trademark Office; Copyright 2003 by the American Chemical Society

## Solvation Dynamics and Proton Transfer in Supramolecular Assemblies

KANKAN BHATTACHARYYA\*

Department of Physical Chemistry, Indian Association for the Cultivation of Science, Kolkata 700 032, India

Received June 25, 2002

### ABSTRACT

Water molecules confined in a supramolecular assembly control reactivity and dynamics of biological systems in a unique way. In a confined system, water molecules display an ultraslow component of solvation which is slower than that in bulk water by 2–4 orders of magnitude. The ultraslow component arises mainly from the disruption of the hydrogen-bond network of water and the binding of water molecules to a macromolecule. The ultraslow component of solvation markedly retards polar reactions. Many examples of slow dynamics in complex systems, and their implications in biological and natural processes are discussed.

### Introduction

In many supramolecular assemblies, water molecules remain confined in a small volume. There is a burgeoning interest to understand how the confined water molecules control structure, reactivity, molecular recognition, and dynamics in a biological system. Water is crucial in self-assembly of molecules, and the exotic structures (Figure 1) arises primarily from an interplay between the hydrophobic and the hydrophilic interactions.<sup>1</sup> Such nanostructures are central in molecular recognition,<sup>1</sup> drug delivery,<sup>2</sup> and nanometer sized electronic devices.<sup>3</sup>

In an attempt to unravel dynamics in these assemblies, there have been many recent studies using ultrafast laser

Kankan Bhattacharyya was born in 1954. He carried out Ph.D. research at the Indian Association for the Cultivation of Science (IACS). After working at the Radiation Laboratory, University of Notre Dame, and at Columbia University, he joined the IACS in 1987. His interests include supramolecular assemblies and ultrafast lasers.

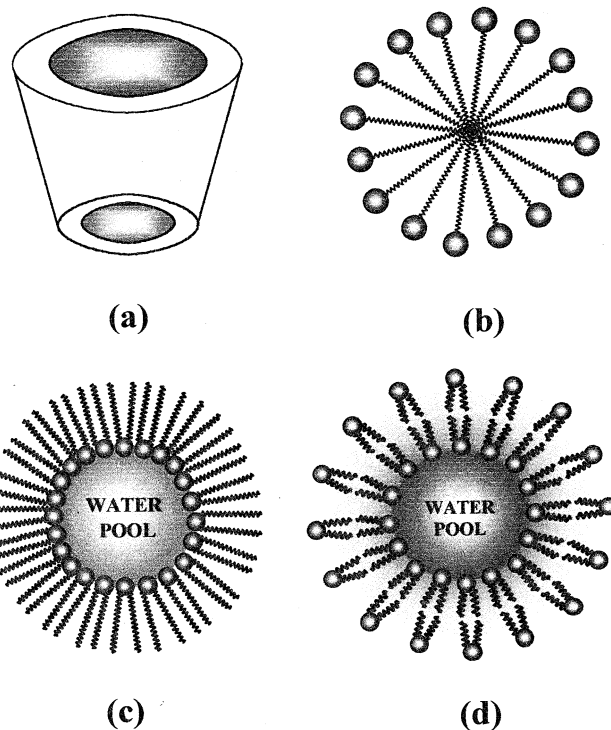
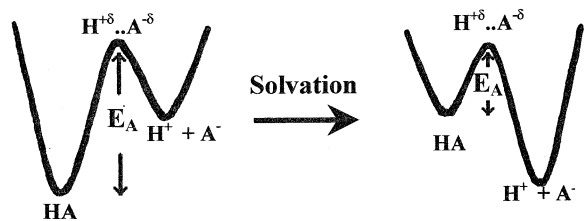


FIGURE 1. Structure of some supramolecular assemblies: (a) cyclodextrin, (b) micelle, (c) microemulsion, and (d) lipid vesicles.

spectroscopy,<sup>4–6</sup> dielectric relaxation,<sup>7</sup> and molecular dynamic simulations.<sup>11</sup> The most interesting observation has been the discovery of an ultraslow component of solvation dynamics in many supramolecular assemblies which is slower than that in bulk water by 2–4 orders of magnitude.<sup>4,5</sup> This demonstrates that the water molecules confined in a supramolecular assembly are fundamentally different from bulk water.

The most important consequence of the ultraslow component of solvation is a marked retardation of a polar reaction in a supramolecular assembly. The retardation is caused by the insufficient and incomplete solvation of the polar transition state by the confined water molecules. As a result of this, the activation barrier in a confined system is much higher than that in a polar solvent (Figure 2). For water (and many other polar solvents), the solva-



Nonpolar solvent

Polar solvent

FIGURE 2. Effect of solvation on the dissociation of an acid,  $\text{HA} \rightarrow \text{H}^+ + \text{A}^-$ .

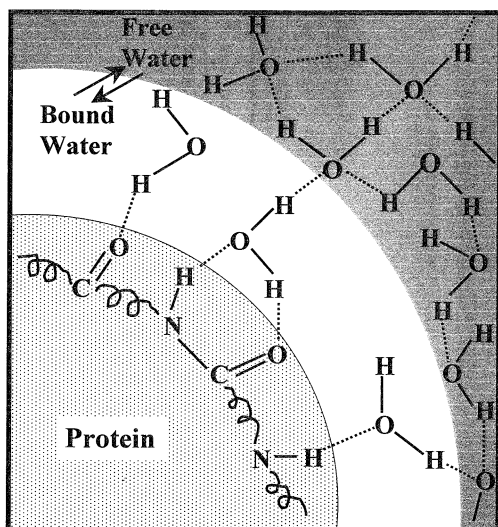


FIGURE 3. "Free" and "bound" water in the hydration shell of a protein.

tion time in bulk is 1–10 ps.<sup>8–10</sup> This is faster than many chemical reactions. However, in many confined systems, solvation dynamics of water molecules exhibits a dramatically slow component of 100–10000 ps.<sup>4,5</sup> If a particular reaction occurs in 10–100 ps in bulk water, solvation remains incomplete, and the reaction will be markedly retarded in a supramolecular assembly. One such reaction is the dissociation of the acid 1-naphthol, which occurs in 35 ps in bulk water. In this account, we will discuss several examples of slow solvation in supramolecular assemblies and its effect on dissociation of 1-naphthol.

Nandi and Bagchi coined the term biological water to describe the water molecules in the vicinity of a biological macromolecule.<sup>12</sup> They proposed that in a biological system there are two kinds of water molecules—"bound" and "free" (Figure 3).<sup>12</sup> The bound water molecules are those which are almost completely immobilized because of attachment to a macromolecule by 1–2 hydrogen bonds. The free water molecules are located at a distance from the macromolecules. They retain the 3-dimensional hydrogen bond network present in bulk water and are very fast (Figure 3). Bagchi et al. suggested that the slow component of solvation arises from the interconversion between bound and free water molecules.<sup>11,12</sup>

**Solvation Dynamics.** In a solvation dynamics experiment, one studies the dynamics of solute–solvent interac-

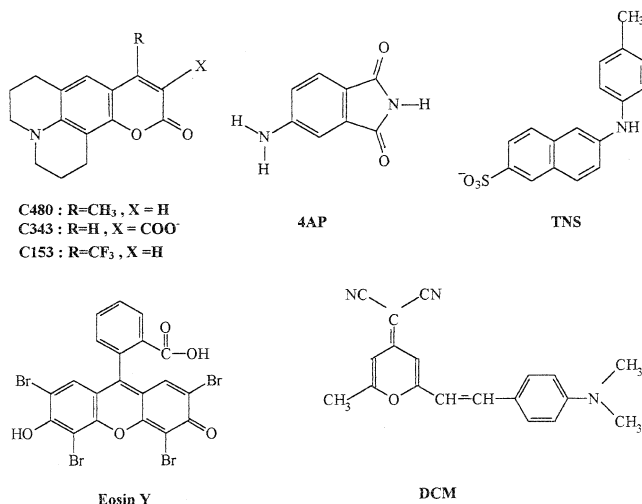


FIGURE 4. Structure of a few solvation probes.

tion i.e., how quickly the solvent dipoles rearrange around a solute dipole created in a polar liquid. For this experiment, one uses a solute whose dipole moment is nearly zero in the ground state but is very large in the excited state. Structures of some solvation probes are shown in Figure 4. When such a solute molecule is in its ground state, the solvent dipoles remain randomly arranged (Figure 5). On excitation of the solute by an ultrashort light pulse, a dipole is created suddenly. Immediately after creation of the solute dipole, the solvent dipoles are randomly oriented and the energy of the system is high (Figure 5). With increase in time, as the solvent dipoles reorient, the energy of the solute dipole decreases and its fluorescence maximum gradually shifts to lower energy i.e., toward longer wavelength. This is known as time dependent fluorescence Stokes shift (TDFSS). Evidently, at a short wavelength, the fluorescence corresponds to the unsolvated solute and exhibits a decay. At a long wavelength, the fluorescence originates from the solvated species and a rise precedes the decay. The rise at a long wavelength corresponds to the formation of the solvated species and, hence, is a clear manifestation of solvation dynamics. To illustrate this, fluorescence decays of a probe (TNS) bound to a polymer–surfactant aggregate at various wavelengths are shown in Figure 6.

Solvation dynamics is described by the decay of the time correlation function  $C(t)$  which is defined as

$$C(t) = \frac{\nu(t) - \nu(\infty)}{\nu(0) - \nu(\infty)} \quad (1)$$

where  $\nu(0)$ ,  $\nu(t)$ , and  $\nu(\infty)$  denote the observed emission energies (frequencies) at time zero,  $t$ , and infinity, respectively. Obviously,  $\nu(0) > \nu(t) > \nu(\infty)$ . At  $t = 0$ , the value of  $C(t)$  is one, and at  $t = \infty$  it is zero.

The continuum model predicts that the solvation time  $\tau_s$  is  $(\epsilon_\infty/\epsilon_0)\tau_D$ , where  $\epsilon_\infty$  and  $\epsilon_0$  are, respectively, the high-frequency and static dielectric constants of the solvent and  $\tau_D$  is the dielectric relaxation time.<sup>10</sup> For water,  $\tau_D$  is 8.3 ps, while  $\epsilon_\infty$  and  $\epsilon_0$  are, respectively, about 5 and 80.<sup>10</sup> Thus, the solvation time of water is 0.5 ps. Barbara et al.<sup>11</sup>

\* E-mail: pckb@mahendra.iacs.res.in. Fax: (91) 33-473-2805.

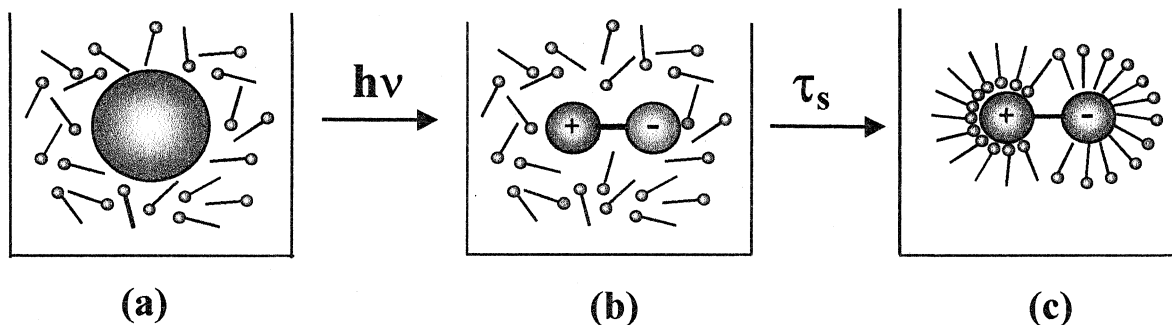


**FIGURE 5.** Solvation dynamics: arrangement of solvent dipoles (match sticks) (a) before excitation of the solute and (b) immediately after creation of the dipole by excitation of the solute. (c) Fully solvated solute dipole.

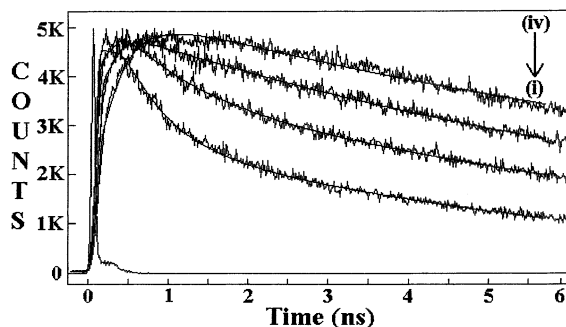


**FIGURE 6.** Fluorescence decays of TNS in a PVP-SDS aggregate at (i) 390, (ii) 420, (iii) 450, and (iv) 530 nm.

observed that the solvation dynamics in water is biexponential with two components, 0.16 and 1.2 ps. Later, Fleming et al.<sup>12</sup> reported that solvation dynamics in water is described by a Gaussian component of frequency 38.5 ps<sup>-1</sup> and a biexponential decay with components, 126 and 880 fs. Thus, solvation dynamics in bulk water occurs in a <1 ps time scale.

In a supramolecular assembly, a substantial fraction of the confined water molecules remains bound to the macromolecules by hydrogen bond and electrostatic attraction. In the following sections, we will describe how confined water molecules causes a very long solvation time in a 100–1000 ps time scale. We will then briefly outline the current theoretical understanding of the slow dynamics, and finally, we will discuss how it affects proton-transfer processes.

#### Solvation Dynamics in Supramolecular Assemblies.

**a. Cyclodextrins.** A cyclodextrin is an interesting host molecule with a cavity (height 8 Å and diameter 4.5–8 Å, Figure 1a) which can encapsulate a guest molecule along with several solvent molecules, and thus, a cyclodextrin serves as a nanovessel for chemical reactions. Cyclodextrins are soluble in water and more soluble in many other polar solvents such as formamide, dimethylformamide, and dimethyl sulfoxide. Fleming et al. studied solvation dynamics of water confined in a  $\gamma$ -cyclodextrin cavity and detected three very slow components of 13, 109, and 1200 ps.<sup>13</sup> Sen et al. studied solvation dynamics of a nonaqueous solvent, dimethylformamide in a  $\beta$ -cyclodextrin cavity.<sup>14</sup> The dynamics of confined dimethylformamide molecules is found to be described by two slow components of 400 and 8000 ps (Table 1).<sup>14</sup> This is substantially slower than the solvation ( $\sim$ 1 ps) in bulk dimethylformamide.<sup>10</sup>

**Table 1. Solvation Times in Different Organized Assemblies**

medium	probe	solvation time (ps)
$\beta$ -cyclodextrin/DMF <sup>a</sup>	4-AP	400 (25%), 8000 (75%)
TX micelle <sup>b</sup>	DCM	300 (15%), 2440 (85%)
CTAB micelle <sup>b</sup>	DCM	170 (50%), 630 (50%)
SDS micelle <sup>b</sup>	DCM	160 (55%), 2900 (45%)
bile salt <sup>c</sup>	DCM	110 (19%), 700 (17%), 2750 (64%)
AOT microemulsion <sup>d</sup>	DCM	280 (55%), 2400 (45%)
PVP-SDS aggregate <sup>e</sup>	TNS	300 (55%), 2500 (45%)
protein (HAS) <sup>f</sup>	DCM	600 (25%), 10,000 (75%)
sol-gel <sup>g</sup>	C480	120 (85%), 800 (15%)

<sup>a</sup> Ref 14. <sup>b</sup> Ref 15. <sup>c</sup> Ref 19. <sup>d</sup> Ref 22. <sup>e</sup> Ref 29. <sup>f</sup> Ref 34. <sup>g</sup> Ref 39.

This demonstrates solvation dynamics of both water and dimethylformamide are significantly inhibited inside a cyclodextrin cavity. Nandi and Bagchi ascribed the slow dynamics inside cyclodextrin cavity to almost complete suppression of the translational modes of the trapped water molecules in the  $\gamma$ -CD cavity.<sup>15</sup>

**b. Micelles.** Micelles (Figure 1b) are spherical aggregates of surfactants with a “dry” hydrocarbon core and a polar peripheral shell which contains polar/ionic headgroups, counterions, and the water molecules forming hydrogen bond bridges between the surfactant molecules. Solvation dynamics of the water molecules hydrogen bonded to the polar headgroups of a micelle exhibit a very slow component in a 100–1000 ps time scale.<sup>4,5,11,16</sup> Solvation times in different micelles are listed in Table 1. The difference in the solvation times has been ascribed to the structures of the micelles. For the neutral surfactant, Triton X-100 (TX) the hydration (palisade) layer is quite thick (20 Å) so that the probe is completely shielded from bulk water. In the case of ionic micelles (cetyl trimethylammonium bromide, CTAB, and sodium dodecyl sulfate, SDS), the hydration (Stern) layer is quite thin (6–9 Å). As a result, in the Stern layer of an ionic micelle, the probe remains partially exposed to bulk water and hence, display fast dynamics.<sup>4–5,16</sup>

The ultrafast components of solvation dynamics in a micelle are detected in a recent femtosecond upconversion study.<sup>17</sup> The solvation dynamics is found to be described by components of 2.1, 165, and 2050 ps for TX and 0.23, 6.5 (average 1.75 ps), and 350 ps for CTAB.<sup>17</sup>

Hara et al.<sup>18</sup> studied the effect of high pressure on the solvation dynamics of C153 in TX micelle. They observed that the solvation dynamics is bimodal with one component in a 150–200 ps time scale and another in a 1000–



2000 ps time scale. With increase in the pressure, the solvation dynamics becomes faster. This is attributed to the weakening of hydrogen bonds with pressure.

The bile salt, sodium deoxycholate (NaDC) is a natural amphiphile which exhibits two critical micellar concentrations at  $\sim 10$  mM ( $\text{CMC}_1$ ) and  $\sim 60$  mM ( $\text{CMC}_2$ ). Above  $\text{CMC}_1$ , bile salts form primary aggregates with the hydrophilic groups pointing outward.<sup>19</sup> Above  $\text{CMC}_2$ , secondary aggregates are formed which resemble an elongated rod, with a central hydrophilic core filled with water and the ions. The solvation dynamics of DCM in a secondary aggregate of NaDC is found to be triexponential with components of 110, 700, and 2750 ps (Table 1).<sup>20</sup> These components are significantly slower than those in bulk water.

*c. Reverse Micelles and Microemulsions.* In a microemulsion, the water molecules exist as a nanometer sized droplet, called a “water pool.” The water pool is surrounded by a layer of surfactant molecules whose polar headgroups point inward (Figure 1c).<sup>4–6,21–22</sup> The water pool in a microemulsion is an elegant model of confined water molecules. For the surfactant, AOT (sodium dioctyl sulfosuccinate) radius of the water pool is approximately  $2w_0$  (Å), where  $w_0$  denotes the water to surfactant molar ratio. In a water pool with  $w_0 > 10$ , solvation dynamics of water exhibits a component in a 100–1000 ps time scale, which is slower by 3 orders of magnitude compared to bulk water.<sup>4–6,23</sup>

Solvation dynamics of C343 in AOT microemulsion has been studied in near-critical propane at 100 bar pressure and is found to be similar to that in an ordinary hydrocarbon at ambient pressure.<sup>24</sup> This shows that pressure does not affect the internal water pool but affects only the droplet–droplet interaction.

Addition of a polymer polyvinylpyrrolidone (PVP) to the water pool affects the size of the surfactant assembly and solvation dynamics.<sup>25</sup> Hydrodynamic diameter of the surfactant assembly increases from 24 nm at 0 wt % PVP to 62 nm at 0.75 wt % PVP and then decreases to 31 nm at 2.5 wt % PVP.<sup>25</sup> The average solvation time is 350 ps in 0%, 115 ps in 0.75 wt %, and 2500 ps in 2.5 wt % PVP.<sup>25</sup> It is proposed that in 0.75% PVP, solvation dynamics is fast because of the large size of the pool. For 2.5 wt % PVP, there are 16 polymer particles of diameter 3.2 nm in each pool of diameter 31 nm, and this makes the motion of the water molecules highly restricted in the pool.<sup>25</sup>

*d. Lipids.* A lipid vesicle resembles a biological cell. A vesicle is an aqueous volume (“water pool”) entirely enclosed by a membrane and dispersed in bulk water (Figure 1d). Molecular dynamics simulations indicate that in a vesicle each surfactant molecule forms hydrogen bond to 4–5 water molecules and about 70% of the surfactant molecules are connected by hydrogen bond bridges.<sup>26</sup> Hof et al.<sup>27</sup> used time-resolved fluorescence and NMR to study solvent relaxation in lipids. Bhattacharyya et al.<sup>28</sup> demonstrated that the solvation dynamics in lipid vesicles is biexponential with one component of a few hundred picoseconds and another of several thousand picoseconds. The slow solvation dynamics clearly demonstrates that the

motion of the water molecules is highly constrained in the inner water pool of the vesicles.

*e. Polymer and Polymer–Surfactant Aggregates.* A polymer–surfactant aggregate is a simple model system to study interaction between two complex systems and formation of new structures.<sup>29</sup> In a polymer–surfactant aggregate, the surface of the micelle remains shielded from bulk water by the polymer chains. The structure of such an aggregate resembles a “necklace” with spherical micelles as beads and polymer chains as connecting threads.

The solvation dynamics in a polymer–surfactant aggregate is found to be appreciably slower than that in a micelle or in an aqueous solution of the polymer.<sup>30,31</sup> Solvation dynamics of TNS in PVP–SDS aggregate is described by two components, 300 and 2500 ps (Table 1).<sup>30</sup> In contrast, solvation dynamics of TNS occurs in  $< 50$  ps in SDS micelles, while in an aqueous solution of PVP the solvation dynamics is described by a major (85%) component of 60 ps.<sup>30</sup> The slower solvation dynamics in PVP–SDS aggregate compared to the polymer PVP alone or SDS alone indicates severe restrictions on the mobility of the water molecule squeezed between the polymer chains and the micellar (SDS) surface.<sup>30</sup>

Castner et al.<sup>32</sup> studied solvation dynamics in aqueous solution of an amphiphilic starlike macromolecule (ASM) which consists of a hydrophobic core and a peripheral hydrophilic shell. The solvation dynamics in ASM is described by an ultrafast component of 0.95 ps (44%) and two very slow components of 361 ps (19%) and 3962 ps (37%).<sup>32</sup> Shirota and Castner<sup>33</sup> studied aqueous polyacrylamide solutions and detected ultrafast reorientation dynamics of the polymer segments with the longest component in 4–10 ps time scale.

*f. Proteins and DNA.* Water molecules at the surface of a protein direct many highly specific binding processes (e.g., enzyme–substrate, antibody–antigen binding, etc.), and thus, they act as ushers in the molecular recognition process. Fleming et al. studied dynamics of a noncovalent probe, eosin in the hydration layer of a protein (lysozyme) using three photon echo peak shift.<sup>34</sup> They detected a very long component of 530 ps which is absent for free eosin in bulk water. This demonstrates that the water molecules in the immediate vicinity of the protein are highly constrained. Solvation dynamics of a noncovalent probe (DCM) in human serum albumin exhibits two components of 600 and 10 000 ps.<sup>35</sup> Zewail et al. observed that solvation dynamics of a noncovalent and a covalent probe in a protein (histone) is similar to bulk water.<sup>36</sup> Solvation dynamics of the intrinsic probe, tryptophan occurs in  $< 1.1$  ps in bulk water time scale, while a long component of 38 ps is detected in a protein, Subtilisin Carlsberg (SC).<sup>37</sup> Interestingly, when a probe (dansyl) resides at a distance of 7.5 Å from the surface of the same protein (SC), the long component (38 ps) vanishes, and the solvation dynamics resembles bulk water.<sup>37</sup> For another covalent probe buried about 5 Å below a protein surface two components of 40 and 580 ps are reported.<sup>38</sup> Thus, solvation dynamics depends markedly on the distance of the water molecules from the protein surface.

Brauns et al. studied solvation dynamics in DNA using a covalently attached probe and detected logarithmic relaxation from 40 ps to 40 ns.<sup>39</sup> They ascribed this to the presence of large number of conformational substates.

*g. Nanoporous Material: Zeolite and Sol–Gel Glass.* In the supercages of a faujasite zeolite 13X, nanosecond solvation dynamics is observed in the absence of a solvent and has been ascribed to the motion of the sodium ions.<sup>40</sup> Optical Kerr effect studies on various liquids confined in a sol–gel glass reveal a major bulklike component and an additional component which is nearly 4 times slower.<sup>41</sup> In a sol–gel glass with 10 Å pores, the average solvation time of trapped water molecules is found to be 220 ps.<sup>42</sup> This is about 200 times slower than that in bulk water. The average solvation time of ethanol in bulk is 12.5 ps, while it is 18.6 ps in a sol–gel glass with 75 Å pores and 35.9 ps in 50 Å pores.<sup>43</sup> In polyacrylamide hydrogel with very big pores, the solvation dynamics is observed to be very fast (<50 ps).<sup>44</sup>

*h. Air–Water Interface.* Eisenthal et al. studied solvation dynamics at the water surface using surface second harmonic generation.<sup>45,46</sup> They reported that at the water surface solvation dynamics occurs in subpicosecond time scale and that the dynamics depends on solute orientation<sup>45</sup> and presence of surfactants.<sup>46</sup>

#### Origin of the Slow Component of Solvation Dynamics.

The very long component of the solvation dynamics in 1000 ps time scale may be explained semiquantitatively as follows. For many organized assemblies, the dielectric relaxation time ( $\tau_D$ ) is about 10 ns, while the dielectric constant ( $\epsilon_0$ ) of confined water is close to that of alcohol (i.e., about 30).<sup>45</sup> If we assume that the high-frequency dielectric constant ( $\epsilon_\infty$ ) in a supramolecular assembly is same as that in water, according to the continuum model the solvation time is  $(5/30) \times 10$  ns or about 1600 ps.

To examine the role of translational diffusion, the coefficient for translational diffusion ( $D$ ) of fluorescent probes in several organized assemblies have been recently determined using decay of fluorescence anisotropy.<sup>47</sup>  $D$  of organic molecules in micelles and polymer–surfactant aggregates (about  $10^{-10}$  m<sup>2</sup> s<sup>-1</sup>)<sup>47</sup> are very similar to that of an organic molecule in bulk water.<sup>48</sup> Thus, the translational diffusion of the probe has little or no role in the dramatic slowing down of solvation dynamics in organized assemblies.

According to the recent theoretical studies, the ultraslow component of solvation dynamics in organized assemblies originates to a large extent from the disruption of the hydrogen bond network of water. In the liquid phase, water molecules in close proximity mutually polarize each other. This results in an increase in the dipole moment of water from 1.85 D in the vapor to 2.6 D in the liquid phase. Berne et al.<sup>49</sup> showed that the high binding energy and dielectric constant of liquid water arise because of the large contribution of the polarization effect. In an organized assembly, the polarization of a water molecule by the neighboring water molecules is prevented. This causes a marked decrease in the dielectric constant of water in a confined environment.

A water–biomolecule hydrogen bond is stronger than a water–water hydrogen bond. Thus, the bound water molecules are more stable than the free water molecules.<sup>12,50</sup> The slow dielectric relaxation results from a dynamic exchange between bound and free water. The slow component depends on the free energy difference ( $\Delta G^\circ$ ) between bound and free water molecules.<sup>12,50</sup> Nandi and Bagchi showed that the slow relaxation component varies from 35 ps (for  $\Delta G^\circ = -1.4$  kcal mol<sup>-1</sup>) to 2857 ps (for  $\Delta G^\circ = -4$  kcal mol<sup>-1</sup>).<sup>12</sup>

There are many computer simulations on dynamics in complex assemblies. Stillinger et al. reported that a water molecule in the first solvation shell of a hydrophobic solute is 20% slower than that in bulk.<sup>51</sup> The segmental motion of the polyethers was found to give rise to a 100 ps component of solvation dynamics.<sup>52</sup> Michael and Benjamin<sup>53</sup> demonstrated that the solvation dynamics at a liquid–liquid interface exhibits a slow component which is absent in bulk water or at the water–vapor interface.

Balasubramanian and Bagchi carried out a simulation of the hydrogen bond dynamics,<sup>11</sup> solvation,<sup>54</sup> and orientational dynamics<sup>55</sup> at the surface of a micelle. The decay of  $C(t)$  at the micellar surface<sup>54</sup> may be fitted to a triexponential function having components, 1.6, 4.3, and 30 ps. The ultrafast components (1.6 and 4.3 ps) detected in this simulation<sup>54</sup> are close to the experimental values.<sup>17</sup> The most recent simulation suggests that the lifetime of the hydrogen bond between a water molecule and the polar headgroup of a micelle is about 13 times slower than that of a water–water hydrogen bond and the activation barrier for interconversion of bound to free water in a micelle is 3.5 kcal/mol.<sup>11</sup>

For a microemulsion, Faeder and Ladanyi<sup>56</sup> carried out a simulation up to 10 ps and hence, did not detect the slow dynamics in a 100–1000 ps time scale. Senapati and Chandra<sup>57</sup> showed that the dielectric constant and solvation time inside a microemulsion is lower than that in bulk water by less than 1 order of magnitude.

**Excited-State Proton Transfer in a Supramolecular Assembly: Effect of Slow Solvation.** The simplest example of a polar reaction is the dissociation of an acid,  $\text{HA} \rightarrow \text{H}^+ + \text{A}^-$  (Figure 2). In a nonpolar medium, this process is endothermic and is unfavorable because of high activation energy. However, in a polar solvent the dissociation of the acid becomes favorable because of the solvation of the transition state. We will now discuss how the slow solvation dynamics affects this process in a supramolecular assembly.

For this purpose, we have used 1-naphthol as probe. 1-Naphthol is a weak base in the ground state ( $\text{p}K_a = 9.5$ ). But in the first excited state, its  $\text{p}K_a^*$  decreases by 9 units to 0.5. Thus, 1-naphthol is a strong photoacid, i.e., a molecule which becomes an acid on excitation by a photon.<sup>58,59</sup> The excited state proton transfer (ESPT) of 1-naphthol occurs if the solvent sufficiently stabilizes the polar TS and the products (i.e. proton and anion). ESPT of 1-naphthol occurs in a water cluster in a supersonic jet only if there are at least 30 water molecules in the cluster.<sup>60</sup> However, ESPT of 1-naphthol does not occur

either in a cluster with methanol in supersonic jet or in a liquid solution in methanol.<sup>60</sup> It is proposed that methanol does not cause adequate solvation of 1-naphthol because of steric hindrance.<sup>60</sup>

Dynamics of ESPT of 1-naphthol is monitored by the decay of the emission from the neutral form (at 360 nm) and the rise of the anion emission (at 460 nm). In aqueous solution, ESPT of 1-naphthol occurs in 35 ps.<sup>59</sup> The slow and inadequate solvation in an organized assembly results in a marked retardation of the ESPT process of 1-naphthol in the nanocavity of cyclodextrin,<sup>61</sup> in micelles,<sup>62</sup> and in a polymer–surfactant aggregate.<sup>63,64</sup>

Inside a  $\beta$ -CD cavity ESPT of 1-naphthol occurs in 930 ps.<sup>61</sup> In micelles, ESPT of 1-naphthol is very slow. The rise times of the anion emission of 1-naphthol in CTAB, SDS, and Triton-X 100 (reduced) (TX-100R) micelles are, respectively, 600, 600, and 1900 ps.<sup>63</sup> In PVP–SDS aggregate, two sites are detected.<sup>61</sup> 88% of the 1-naphthol molecules reside in a site where ESPT is totally blocked giving rise to a very long component of decay (5300 ps) of the neutral form.<sup>63</sup> In the other site, 1-naphthol molecules undergo ESPT in 1600 ps time scale. This component appears in the decay of the neutral emission and in the rise of the anion emission.<sup>63</sup>

Apart from solvating the transition state, the solvent affects diffusional separation and geminate recombination of the anion ( $A^-$ ) and the proton. This leads to a nonexponential decay even in water.<sup>58</sup> Recently, Huppert et al. extended this analysis to a reverse micelle and studied diffusion and ESPT in a water pool.<sup>65</sup>

## Conclusion and Future Outlook

The ultimate goal of ultrafast spectroscopy is to develop a comprehensive picture of dynamics in biological assemblies and to explain why chemistry in a confined environment is so different from that in an ordinary solution. The surprisingly slow component of solvation dynamics has very serious biological implications. The finding that slow solvation causes slow proton transfer is extremely relevant in electron transfer and other polar reactions occurring in biological assemblies.

One of the future challenges would be to explain site-specific chemistry in a biological system by studying many more proteins using covalent probes at selected locations.<sup>37–39</sup> A biological assembly is quite flexible so that it can capture the reactants, position them in proper geometry, and, finally, release the products. It is still not known how solvation dynamics changes when a biological system undergoes such structural transitions. The interaction between a polymer and a surfactant may be a good model to study this issue. This should eventually lead to a deeper understanding of enzyme catalysis. It will be interesting to know the difference in the solvation dynamics in a folded and an unfolded protein. This would elucidate the exact role of water in protein folding.

Apart from solvation dynamics and proton transfer, the hydrogen bond network of water plays a key role in many other phenomena, e.g., freezing.<sup>66</sup> Disruption of the

hydrogen bond network affects freezing of water. The water molecules attached to some macromolecules do not freeze even at  $-30^\circ\text{C}$ . Unfrozen water molecules help to sustain many organisms and plants at sub-zero temperatures.

In summary, constrained water in a supramolecular assembly profoundly influence a large number of natural phenomena, and hence, unraveling its mystery may have far reaching consequences.

*I thank Department of Science and Technology for generous grants. It is a pleasure to thank Professor B. Bagchi for many illuminating discussions and Professor G. R. Desiraju for his kind interest. Finally, I thank all my students for their enthusiasm and active participation in the works described in this article.*

## References

- Selinger, J. V.; Spector, M. S.; Schnur, J. M. Theory of self-assembled tubules and helical ribbons. *J. Phys. Chem. B* **2001**, *105*, 7157–7169.
- Muller, A.; O'Brien, D. F. Supramolecular materials via polymerization of mesophases of hydrated amphiphiles. *Chem. Rev.* **2002**, *102*, 727–758.
- Xia, Y.; Rodgers, J.; Paul, K. E.; Whitesides, G. M. Unconventional methods for fabricating and patterning nanostructures. *Chem. Rev.* **1999**, *99*, 1823–1848.
- Nandi, N.; Bhattacharyya, K.; Bagchi, B. Dielectric relaxation and solvation dynamics of water in complex chemical and biological Systems. *Chem. Rev.* **2000**, *100*, 2013–2045.
- Bhattacharyya, K.; Bagchi, B. Slow dynamics of constrained water in complex geometries. *J. Phys. Chem. A* **2000**, *104*, 10603–10613.
- Levinger, N. E. Ultrafast dynamics in reverse micelles, microemulsions, and vesicles. *Curr. Opin. Coll. Interface Sci.* **2000**, *5*, 118–124.
- Telgmann, T.; Kaatz, U. Monomer exchange and concentration fluctuations of micelles. Broad band ultrasonic spectrometry of the system triethylene glycol monoethyl ether/water. *J. Phys. Chem. A* **2000**, *104*, 1085–1094.
- Maroncelli, M. The dynamics of solvation in polar liquids. *J. Mol. Liq.* **1993**, *57*, 1–38.
- Jarzeba, W.; Walker, G. C.; Johnson, A. E.; Kahlow, M. A.; Barbara, P. F. Femtosecond microscopic solvation dynamics in aqueous solution. *J. Phys. Chem.* **1988**, *92*, 7039–7041.
- Jimenez, R.; Fleming, G. R.; Kumar, P. V.; Maroncelli, M. Femtosecond solvation dynamics in water. *Nature* **1994**, *369*, 471–473.
- Balasubramanian, S.; Pal, S.; Bagchi, B. Hydrogen bond dynamics near a micellar surface: origin of the universal slow relaxation at complex aqueous interfaces. *Phys. Rev. Lett.* **2002**, *89*, 115505–1–4.
- Nandi, N.; Bagchi, B. Dielectric relaxation of biological water. *J. Phys. Chem. B* **1997**, *101*, 10954–10962.
- Vajda, S.; Jimenez, R.; Rosenthal, S. J.; Fidler, V.; Fleming, G. R.; Castner, E. W., Jr. Femtosecond to nanosecond solvation dynamics in water and inside the  $\gamma$ -cyclodextrin cavity. *J. Chem. Soc., Faraday Trans.* **1995**, *91*, 867–873.
- Sen, S.; Sukul, D.; Dutta, P.; Bhattacharyya, K. Slow solvation dynamics in a nanocavity. 4-Aminophthalimide in cyclodextrin. *J. Phys. Chem. A* **2001**, *105*, 10635–10639.
- Nandi, N.; Bagchi, B. Ultrafast solvation dynamics of an ion in the  $\gamma$ -cyclodextrin cavity: role of restricted environment. *J. Phys. Chem.* **1996**, *100*, 13914–13919.
- Pal, S. K.; Sukul, D.; Mandal, D.; Sen, S.; Bhattacharyya, K. Solvation dynamics of DCM in micelles. *Chem. Phys. Lett.* **2000**, *327*, 91–96.
- Mandal, D.; Sen, S.; Tahara, T.; Bhattacharyya, K. Femtosecond study of solvation dynamics of DCM in micelles. *Chem. Phys. Lett.* **2002**, *359*, 77–82.
- Hara, K.; Kuwabara, H.; Kajimoto, O. Pressure effect on solvation dynamics in micellar environment. *J. Phys. Chem. A* **2001**, *105*, 7174–7179.
- Ju, C.; Bohne, C. Dynamics of probe complexation to bile salt aggregates. *J. Phys. Chem.* **1996**, *100*, 3847–3854.
- Sen, S.; Dutta, P.; Mukherjee, S.; Bhattacharyya, K. Solvation dynamics in bile salt aggregates. *J. Phys. Chem. B* **2002**, *106*, 7745–7750.
- Venables, D. S.; Huang, K.; Schmuttenmaer, C. A. Effect of reverse micelle size on the librational band of confined water and methanol. *J. Phys. Chem. B* **2001**, *105*, 9132–9138.



- (22) Brubach, J.-B.; Mermut, A.; Filabozzi, A.; Gerschel, A.; Lairez, D.; Kraft, M. P.; Roy, P. Dependence of water dynamics upon confinement size. *J. Phys. Chem. B* **2001**, *105*, 430–435.
- (23) Pal, S. K.; Mandal, D.; Sukul, D.; Bhattacharyya, K. Solvation dynamics of 4-(dicyano-methylene)-2-methyl-6-(p-dimethylamino-styryl)-4H-pyran (DCM) in a microemulsion. *Chem. Phys. Lett.* **1999**, *312*, 178–184.
- (24) Bhattacharyya, K.; Hara, K.; Kometani, N.; Yozu, Y.; Kajimoto, O. Solvation dynamics in a microemulsion in near-critical propane. *Chem. Phys. Lett.* **2002**, *361*, 136–142.
- (25) Sen, S.; Sukul, D.; Dutta, P.; Bhattacharyya, K. Solvation dynamics in the water pool of AOT microemulsions. Effect of Polymer. *J. Phys. Chem. A* **2002**, *106*, 6017–6023.
- (26) Pasenkiewicz-Gierula, M.; Takaoka, V.; Miyagawa, H.; Kitamura, K.; Kusumi, A. Hydrogen-bonding of water to phosphatidylcholine in the membrane as studied by molecular dynamics simulations: location, geometry and lipid–lipid bridging via hydrogen bonded water. *J. Phys. Chem. A* **1997**, *101*, 3677–3691.
- (27) Sykora, J.; Kapusta, P.; Fidler, V.; Hof, M. On what time scale does solvent relaxation in phospholipid bilayers happen? *Langmuir* **2002**, *18*, 571–573.
- (28) Pal, S. K.; Sukul, D.; Mandal, D.; Bhattacharyya, K. Solvation dynamics of DCM in lipid. *K. J. Phys. Chem. B* **2000**, *104*, 4529–4531.
- (29) Narenberg, R.; Kliger, J.; Horn, D. Study of interactions of poly(vinylpyrrolidone) and sodium dodecyl sulfate by fluorescence correlation spectroscopy. *Angew. Chem., Int. Ed. Engl.* **1999**, *38*, 1626–1629.
- (30) Sen, S.; Sukul, D.; Dutta, P.; Bhattacharyya, K. Solvation dynamics in aqueous polymer solution and in polymer-surfactant aggregate. *J. Phys. Chem. B* **2002**, *106*, 3763–3769.
- (31) Dutta, P.; Sen, S.; Mukherjee, S.; Bhattacharyya, K. Solvation dynamics of TNS 540 in polymer (PEG)-surfactant (SDS) aggregate. *Chem. Phys. Lett.* **2002**, *359*, 15–21.
- (32) Frauchiger, L.; Shirota, H.; Uhrich, K. E.; Castner, E. W. Jr. Dynamic fluorescence probing of the local environments within amphiphilic star-like macromolecules. *J. Phys. Chem. B* **2002**, *106*, 7463–7468.
- (33) Shirota, H.; Castner, E. W. Jr. Ultrafast dynamics in aqueous polyacrylamide solutions. *J. Am. Chem. Soc.* **2001**, *123*, 12877–12885.
- (34) Jordandies, X. J.; Lang, M. J.; Song, X.; Fleming, G. R. Solvation dynamics in protein environments studied by photon echo spectroscopy. *J. Phys. Chem. B* **1999**, *103*, 7995–8005.
- (35) Pal, S. K.; Mandal, D.; Sukul, D.; Sen, S.; Bhattacharyya, K. Solvation dynamics of DCM in human serum albumin. *J. Phys. Chem. B* **2001**, *105*, 1438–1441.
- (36) Zhong, D.; Pal, S. K.; Zewail, A. H. Femtosecond studies of protein-DNA binding and dynamics: Histone I. *Chemphyschem* **2001**, *2*, 219–227.
- (37) Pal, S. K.; Peon, J.; Zewail, A. H. Biological water at the protein surface: dynamical solvation probed directly with femtosecond resolutions. *Proc. Natl. Acad. Sci. U.S.A.* **2002**, *99*, 1763–1768.
- (38) Mandal, D.; Sen, S.; Sukul, D.; Bhattacharyya, K.; Mandal, A. K.; Banerjee, R.; Roy, S. Solvation dynamics of a probe covalently bound to a protein and in AOT microemulsion. 4 (N-bromoacetyl-amino)-phthalimide. *J. Phys. Chem. B* **2002**, *106*, 10741–10747.
- (39) Brauns, E. B.; Madaras, M. L.; Coleman, R. S.; Murphy, C. J.; Berg, M. A. Complex local dynamics in DNA on the picosecond and nanosecond time scales. *Phys. Rev. Lett.* **2002**, *88*, 158101-1-4.
- (40) Das, K.; Sarkar, N.; Das, S.; Datta, A.; Bhattacharyya, K. Solvation dynamics in a solid host. Coumarin 480 in Zeolite 13X. *Chem Phys. Lett.* **1996**, *249*, 323–328.
- (41) Loughnane, B. J.; Farrer, R. A.; Scodinu, A.; Reilly, T.; Fourkas, J. T. Ultrafast spectroscopic studies of dynamics of liquids confined in nanoporous glasses. *J. Phys. Chem. B* **2000**, *104*, 5421–5429.
- (42) Pal, S. K.; Sukul, D.; Mandal, D.; Sen, S.; Bhattacharyya, K. Solvation dynamics of coumarin 480 in sol–gel Matrix. *J. Phys. Chem. B* **2000**, *104*, 2613–2616.
- (43) Bauman, R.; Ferrante, C.; Deeg, F. W.; Brauchle, C. Solvation dynamics of Nile blue in ethanol confined in porous sol–gel glasses. *J. Chem. Phys.* **2001**, *114*, 5781–5791.
- (44) Datta, A.; Das, S.; Mandal, D.; Pal, S. K.; Bhattacharyya, K. Fluorescence monitoring of polyacrylamide hydrogel using 4-aminophthalimide. *Langmuir*, **1997**, *13*, 6922–6926.
- (45) Zimdars, D.; Eienthal, K. B. Effect of solute orientation on solvation dynamics at the air/water interface. *J. Phys. Chem. A* **1999**, *103*, 10567–10570.
- (46) Benderskii, A. I.; Eienthal, K. B. Effect of organic surfactants on femtosecond solvation dynamics at the air–water interface. *J. Phys. Chem. B* **2000**, *104*, 11723–11728.
- (47) Sen, S.; Sukul, D.; Dutta, P.; Bhattacharyya, K. Fluorescence anisotropy decay in-polymer-surfactant aggregates. *J. Phys. Chem. A* **2001**, *105*, 7495–7500.
- (48) For instance,  $D_1$  of amino benzoic acid is  $8 \times 10^{-10} \text{ m}^2/\text{s}^{-1}$ : *Handbook of Chemistry and Physics*; CRC Press: Boca Raton, FL, 1990; pp 6–151.
- (49) Rick, S. W.; Stuart, S. J.; Berne, B. J. Dynamical fluctuating charge force fields: applications to liquid water. *J. Chem. Phys.* **1994**, *101*, 6141–6156.
- (50) Nandi, N.; Bagchi, B. Anomalous dielectric relaxation of aqueous protein solutions. *J. Phys. Chem. A* **1998**, *102*, 8217–8221.
- (51) Geiger, A.; Rahman, A.; Stillinger, H. Molecular dynamics simulations of hydration of Lennard-Jones solutes. *J. Chem. Phys.* **1979**, *70*, 263–276.
- (52) Olander, R.; Nitzan, A. Solvation dynamics in dielectric solvents with restricted molecular rotations: Polyethers. *J. Chem. Phys.* **1995**, *102*, 7180–7196.
- (53) Michael, D.; Benjamin, I. Molecular dynamics computer simulations of solvation dynamics at liquid/liquid interfaces. *J. Chem. Phys.* **2001**, *114*, 2817–2824.
- (54) Balasubramanian, S.; Bagchi, B. Slow solvation dynamics near an aqueous micellar surface. *J. Phys. Chem. B* **2001**, *105*, 12529–10533.
- (55) Balasubramanian, S.; Bagchi, B. Slow orientational dynamics of water molecules at a micellar surface. *J. Phys. Chem. B* **2002**, *106*, 3668–3672.
- (56) Faeder, J.; Ladanyi, B. M. Solvation dynamics in aqueous reverse micelles: A computer simulation study. *J. Phys. Chem. B* **2001**, *105*, 11148–11158.
- (57) Senapathy, S.; Chandra, S. Dielectric constant of water in a nanocavity. *J. Phys. Chem. B* **2001**, *105*, 5106–5109.
- (58) Tolbert, L. M.; Solntsev, K. M. Excited-state proton transfer: from constrained systems to “super” photoacids to superfast proton transfer. *Acc. Chem. Res.* **2002**, *35*, 19–27.
- (59) Lee, J.; Robinson, G. W.; Webb, S. P.; Phillips, L. A.; Clark, J. H. Hydration dynamics of protons from photon initiated acids. *J. Am. Chem. Soc.* **1986**, *108*, 6538–6542.
- (60) Saeki, M.; Ishiuchi, S.-I.; Sakai, M.; Fuji, M. Structure of 1-naphthol: alcohol clusters studied by IR dip spectroscopy and *ab initio* molecular orbital calculations. *J. Phys. Chem. A* **2001**, *105*, 10045–10053.
- (61) Hansen, J. E.; Pines, E.; Fleming, G. R. Excited-state proton transfer in 1-aminopyrene complexed with  $\beta$ -cyclodextrin. *J. Phys. Chem.* **1992**, *96*, 6904–6910.
- (62) Mandal, D.; Pal, S. K.; Bhattacharyya, K. Excited-state proton transfer of 1-naphthol in micelles. *J. Phys. Chem. A* **1998**, *102*, 9710–9714.
- (63) Sukul, D.; Pal, S. K.; Mandal, D.; Sen, S.; Bhattacharyya, K. Excited-state proton transfer as a probe for polymer-surfactant interaction. *J. Phys. Chem. B* **2000**, *104*, 6128–6132.
- (64) Dutta, P.; A. Halder, S. Mukherjee, P. Sen, S.; Bhattacharyya, K. Excited-state proton transfer of 1-naphthol in hydroxypropyl-cellulose/sodium dodecyl sulfate. *Langmuir* **2002**, *18*, 7867–7871.
- (65) Cohen, B.; Huppert, D.; Solntsev, K. M.; Tsfadia, Y.; Nachliel, E.; Gutman, M. Excited-state proton transfer in reverse micelles. *J. Am. Chem. Soc.* **2002**, *124*, 7539–7547.
- (66) Ohmine, I.; Saito, S. Water Dynamics: Fluctuation, relaxation and chemical reactions in hydrogen bond network rearrangement. *Acc. Chem. Res.* **1999**, *32*, 741–749.

AR020067M